

Chemical bonding and electronic structure of $R\text{NiO}_3$ ($R = \text{rare earth}$)

J.-S. Zhou and J. B. Goodenough

Texas Materials Institute, ETC 9.102, University of Texas at Austin, 1 University Station, C2201, Austin, Texas 78712, USA

(Received 20 October 2003; revised manuscript received 27 January 2004; published 28 April 2004)

A comparison is made between the local distortions at room temperature of the $MO_{6/2}$ octahedra in three perovskite RMO_3 families in which M is Mn, Fe, or Ni. The comparison distinguishes between distortions arising from cooperative octahedral-site rotation and static Jahn-Teller (JT) distortions. The Mn^{3+} and Fe^{3+} ions have localized $3d$ electrons with primarily ionic M-O bonds whereas the Ni-O bond lengths reflect the crossover from insulator to metallic behavior. Below a critical Ni-O-Ni bond angle, stabilization of two distinguishable $\text{NiO}_{6/2}$ sites is more compatible with the segregation into primarily ionic Ni^{3+} -O bonding at a JT distorted $\text{NiO}_{6/2}$ octahedral site and primarily covalent Ni(III)-O bonding at a less distorted site of smaller mean Ni-O bond length rather than charge transfer between the two Ni sites. Moreover, below a smaller critical M -O- M bond angle, which is the same in all three families, the domination of the M -O- M interaction weakens relative to M -O-O- M next-nearest-neighbor interactions.

DOI: 10.1103/PhysRevB.69.153105

PACS number(s): 71.70.Ej, 71.28.+d, 71.30.+h, 72.80.Ga

The $R\text{NiO}_3$ perovskite family undergoes a transition from metallic behavior with an enhanced Pauli paramagnetism in LaNiO_3 to antiferromagnetic insulating behavior with decreasing size of the R^{3+} ion. An extensive debate concerning the physical origin of the insulator-metal transition found at T_{IM} (see Fig. 1) has remained unresolved. A Mott-Hubbard transition that creates a charge-transfer gap below T_{IM} was proposed early.¹ However, a smooth change of the susceptibility $\chi(T)$ on crossing T_{IM} seems not to support the scenario of a homogeneous Mott transition.² Moreover, Alonso and co-workers³⁻⁷ have taken advantage of neutron diffraction and high-resolution synchrotron x-ray diffraction to go beyond the early observation¹ of a volume contraction on heating through T_{IM} to investigate the local distortions of the $\text{NiO}_{6/2}$ octahedra. They found an ordering of two distinguishable $\text{NiO}_{6/2}$ octahedra, one less distorted with a shorter mean Ni-O bond length $\langle \text{Ni-O} \rangle$ and the other considerably more distorted with a longer $\langle \text{Ni-O} \rangle$. A clear separation into two different octahedral sites sets in below a critical radius of circa 1.075 Å of the R^{3+} ion. This observation has been interpreted in terms of charge disproportionation $2\text{Ni}^{3+} = \text{Ni}^{(3+\delta)+} + \text{Ni}^{(3-\delta)+}$ of the type that has been generally assumed to occur dynamically at $T > T_{\text{JT}} \approx 750$ K in LaMnO_3 , which approaches the insulator-conductor transition from the insulator side.⁸ On the other hand, octahedral distortions in $R\text{NiO}_3$ have been argued by Alonso *et al.*⁴ to be due to the Jahn-Teller (JT) effect.

Normally, charge disproportionation would have to be made at the expense of the on-site Coulomb energy U that splits the $\text{Ni}^{4+}/\text{Ni}^{3+}$ and $\text{Ni}^{3+}/\text{Ni}^{2+}$ redox energies; therefore, it is most likely to occur where U is comparable to the bandwidth W_σ . However, where $W_\sigma \approx U_\sigma$ is found, the lattice may also be unstable relative to a segregation into more covalent and more ionic bonding with a localized t^6e^1 configuration at the larger $\text{NiO}_{6/2}$ site. Moreover, a cooperative JT distortion at the larger $\text{NiO}_{6/2}$ site would further stabilize the localized configuration to increase more the site energy $U_\sigma - W_\sigma$ that would block electron transfer to the larger $\text{NiO}_{6/2}$ site. Whether the charge transfer of a disproportionation reaction occurs depends on the difference in energy of

the t^6e^1 configurations that result from stronger covalent bonding at the smaller $\text{NiO}_{6/2}$ site and the Coulomb energy $U_\sigma - W_\sigma$ at the larger $\text{NiO}_{6/2}$ site. Since a JT distortion is only stabilized where there is an orbital degeneracy, i.e., a t^6e^1 configuration, the observation of a JT deformation at the larger $\text{NiO}_{6/2}$ site would provide a sure experimental distinction between disproportionation and a simple segregation into more ionic and more covalent bonding. By comparing the M -O bond lengths and the local distortions of the $MO_{6/2}$ octahedra in three RMO_3 perovskite families with Mn, Fe, and Ni, we present quantitative criteria for distinguishing not only ionic and covalent bonding, but also the JT distortion from that due to the geometric factor.

Figure 1 presents an overview of the different phases encountered in the $R\text{NiO}_3$ family as a function of temperature and the tabulated room-temperature ionic size of the R^{3+} ion.⁹ The size of the R^{3+} ion determines the magnitude of the geometric tolerance factor $t \equiv (R\text{-O})/[\sqrt{2}(M\text{-O})]$ that is a measure of the mismatch between the equilibrium ($R\text{-O}$) and ($M\text{-O}$) bond lengths of a cubic RMO_3 perovskite. The perovskite structure adjusts to a $t < 1$, which places the $M\text{-O}$ bonds under a compressive stress, by a cooperative rotation of the corner-shared $MO_{6/2}$ octahedra; the rotations bend the $M\text{-O-}M$ bond angle from 180° to a $\theta = (180^\circ - \phi)$ and displace the R^{3+} ion somewhat. The rhombohedral $R\bar{3}c$ structure has the octahedra rotated about a cubic $[111]$ axis; the orthorhombic $Pbnm$ structure has them rotated about a cubic $[110]$ axis. Smaller R^{3+} ions decrease the geometric factor t and transform the $R\bar{3}c$ structure to $Pbnm$. Marezio *et al.*¹⁰ have described the atomic displacements in the orthorhombic $Pbnm$ phase of the $R\text{FeO}_3$ family. Since there is no orbital degeneracy at either a high-spin $\text{Fe}^{3+}:t^3e^2$ configuration or $\text{Gd}^{3+}:4f^7$ configuration, GdFeO_3 serves as a prototype of the orthorhombic distortion that results from octahedral-site rotations alone. The $M\text{-O-}M$ resonance integral b_σ^{cac} for the σ -bonding M - e orbitals is proportional to $\cos \theta$,¹¹ which means that the tight-binding bandwidth for the antibonding σ^* band of e -orbital parentage is $W_\sigma \approx 2z b_\sigma^{\text{cac}} \sim \langle \cos \theta \rangle$ with $z = 6$ nearest like neighbors in an RMO_3 perovskite.

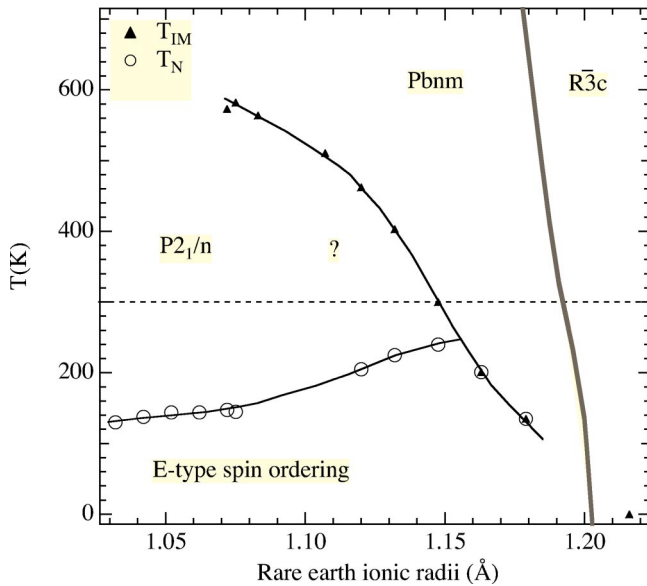


FIG. 1. The phase diagram of $RNiO_3$ (R = rare earth). The data are from Refs. 1, 4, 7, and 25.

Plotted in Fig. 2 are the structure data^{3–7,10,12–17} including the mean bond length $\langle M-O \rangle$ and θ_{av} of RMO_3 ($M = Mn, Fe, Ni$). Even though a wide spreading of θ_{av} due to varying size of R^{3+} is found in magnetic insulators $RFeO_3$ and $RMnO_3$, the $\langle M-O \rangle$ in the $MO_{6/2}$ octahedra are nearly identical and independent of θ_{av} . The ionic bonding range 2.00–2.02 Å for the $\langle M-O \rangle$ in Fig. 2 is almost a perfect fit to the ionic bond lengths of $0.55 + 1.40$ Å for $Fe^{3+}-O^{2-}$ and $0.58 + 1.40$ Å for $Mn^{3+}-O^{2-}$ based on the tabulated ionic radii.⁹ Within the same range of R^{3+} radii, however, the octahedral-site rotations narrow $W_\sigma \sim \langle \cos \theta \rangle$, and lead to the evolution from itinerant toward localized character of the electronic state in $RNiO_3$. Correspondingly, four Ni-O-Ni bonds can be distinguished by the $\langle Ni-O \rangle$ and θ_{av} , as shown in Fig. 2. A smaller $\langle Ni-O \rangle$ of $RNiO_3$ ($R = La, Pr, Nd$) is associated with metallic bonding. The separation into two distinguishable $NiO_{6/2}$ octahedra in the $RNiO_3$ family with smaller θ_{av} creates two different Ni-O bondings; one is close to an ionic bond length $\langle Ni-O \rangle = 0.56 + 1.40$ Å, like the bonding of $\langle Fe-O \rangle$ and $\langle Mn-O \rangle$ for localized $3d^n$ configurations with 3+ valence state; and the other is slightly smaller than the metallic bond in $LaNiO_3$. This observation opens an alternative view to the segregation into two $NiO_{6/2}$ octahedra: *instead of real charge transfer between $NiO_{6/2}$ octahedra, a segregation into ionic and covalent bonding which is made possible by the cooperative oxygen displacements, occurs as θ_{av} is reduced.* The charge disproportionation, if possible, would take place where θ_{av} is close to that of $LaNiO_3$, not in the state where $U-W$ becomes larger. A Jahn-Teller distortion of the larger $NiO_{6/2}$ site, *vide infra*, further verifies the argument of bonding segregation. A significant covalency between $Ni^{3+}:e^1$ and $O^{2-}:2p_\sigma$ orbitals can be achieved at the smaller $NiO_{6/2}$ octahedra, which are slightly smaller than those of $LaNiO_3$. In the range 1.94–1.96 Å, i.e., for the $RNiO_3$ with $R = \langle Ni-O \rangle$ Sm, Eu, Gd, Tb where ordering of smaller and larger $NiO_{6/2}$ octahedra cannot be resolved in the

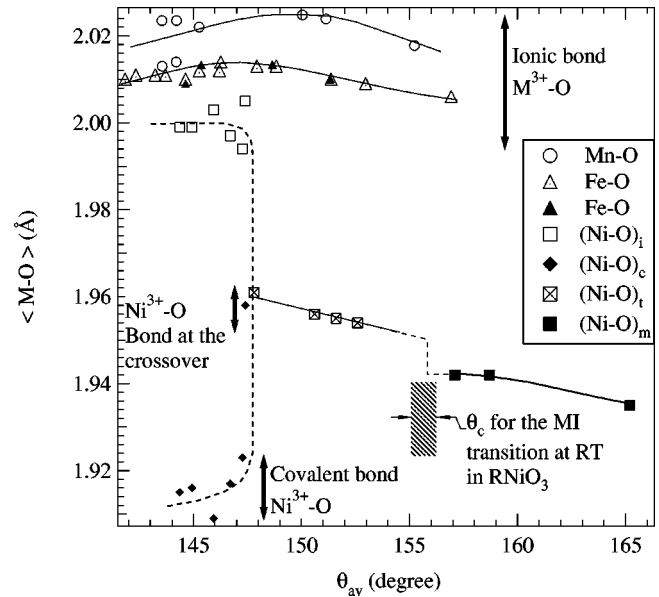


FIG. 2. The average length of the M-O bond at room temperature for RMO_3 ($M = Mn, Fe, Ni$) as a function of the average angle θ_{av} of the M-O-M bond. The $(Ni-O)_i$, $(Ni-O)_c$, $(Ni-O)_t$, and $(Ni-O)_m$ stand for ionic bonding, covalent bonding, the bonding at the crossover and metallic bonding, respectively. The symbol of solid triangle represents structure data of $RFeO_3$ crystals from a synchrotron radiation source (Refs. 14–16). An obvious printing error 0.963 Å of Ni(1)-O1 for $YNiO_3$ (Ref. 6) has been corrected to be 1.963 Å in this plot.

antiferromagnetic insulator phase although it may have the same space group symmetry as that of $YNiO_3$,¹⁸ the $\langle Ni-O \rangle$ reflects a fourth type of bonding. This crossover bond length should not be viewed as a weighted average of ionic and covalent bond lengths; it appears to correspond to a metastable equilibrium state having an intermediate bond length. This room-temperature metastable state gives way to a double-well potential where bond-length ordering occurs at lower values of θ_{av} . The $\langle Ni-O \rangle$ bond length changes discontinuously at the metal-insulator boundary, which occurs at a critical average bond angle θ_c . This small jump corresponds to a discontinuous change of the $\langle Ni-O-Ni \rangle$ bonding that is related to the volume change at the transition. On the other hand, $PrNiO_3$ and $NdNiO_3$ show a suppressed thermal conductivity¹⁹ below T_{IM} , which indicates that the bond-length fluctuations remain. These bond-length fluctuations are only made possible if the Ni-O bond-length potential becomes relatively flat. In the absence of bond-length ordering, bond-length fluctuations and a large bond-length compressibility appear to be important signatures of the crossover. It is also interesting to compare the metal-insulator transition of $RNiO_3$ with that of V_2O_3 . The Mott transition in V_2O_3 leads to a homogeneous change of the electronic state and a major structure change at T_t ,²⁰ whereas an evolution from localized to itinerant electronic behavior in the $RNiO_3$ family as the overlap integral is reduced produces an evolution to the vibronic bonding before exhibiting a phase having 50:50 ionic and covalent bonding.

If the M cations have an e -orbital degeneracy, as is the

case for low-spin $\text{Ni}^{3+}:t^6e^1$ and high-spin $\text{Mn}^{3+}:t^3e^1$, then a distortion of the octahedral site to remove the degeneracy is stabilized at lower temperatures. The degeneracy may be removed by either a tetragonal or an orthorhombic distortion corresponding to a softening of a Q_2 or Q_3 vibrational mode or a linear combination of the two modes. The $Pbnm$ space group and its subspace group $P2_1/n$ used to refine the structure of RNiO_3 ($R = \text{Y, Ho, Lu}$) accommodates a cooperative distortion of the individual $\text{MO}_{6/2}$ octahedra with a linear combination of the Q_2 and Q_3 modes. The JT distortion, which is superimposed on the rotational distortion, is opposed by elastic restoring forces; therefore, the greater the concentration of orbitally degenerate JT ions, the larger the magnitude of the JT component of the distortion. However, an e -orbital degeneracy that leads to a cooperative JT distortion is only found where the e electrons are localized; where they occupy a σ^* band of e orbital parentage, as in LaNiO_3 , there is no cooperative JT distortion, and where the e electrons occupy molecular orbitals as in a covalently bonded $\text{NiO}_{6/2}$ complex, the magnitude of any JT component to the distortion is strongly reduced.

Figure 3 shows the room-temperature parameter $\Delta_d \equiv (1/6)\sum_{n=1,6}[(d_n - \langle d \rangle)/\langle d \rangle]^2$ that measures the magnitude of an octahedral-site distortion obtained from measured literature values of the different Ni-O bond lengths d and also the average M -O- M bond angle θ_{av} as a function of the ionic radius of the R^{3+} ion. The average angle θ_{av} decreases monotonically with the radius of the R^{3+} ion. The distortion parameter Δ_d for the $\text{NiO}_{6/2}$ octahedra remains vanishingly small for the RNiO_3 compounds with $R = \text{La, Pr, Nd}$, that are metallic at room temperature. However, an increase in Δ_d with decreasing size of the R^{3+} ion sets in on crossing T_{IM} , i.e., for $R = \text{Sm, Eu, Gd, ...}$; and for an R^{3+} radius less than 1.08 Å, i.e., $R = \text{Y, Ho, ... Lu}$, two distinguishable $\text{NiO}_{6/2}$ octahedra are observed, the Δ_d for one increasing remarkably while that for the other remains modest. The same result is obtained on crossing T_{IM} with decreasing temperature for a given R^{3+} ion. Nevertheless, the largest Δ_d for the RNiO_3 family is about one order of magnitude smaller than that for the RMnO_3 family shown in Fig. 3(b), which makes it difficult to assert unambiguously that a JT distortion is playing a role in the more distorted $\text{NiO}_{6/2}$ site.

To clarify this issue, Fig. 3(c) shows the Δ_d found in the RFeO_3 family where any distortion can only be due to the octahedral-site rotations. While the Fe-O bond length variation of the $\text{FeO}_{6/2}$ octahedra increases as θ_{av} decreases in a manner analogous to the RMnO_3 and RNiO_3 families, as seen in Fig. 2, Δ_d is a factor of 5 smaller than that of the larger Δ_d of the RNiO_3 family. Moreover, in order to determine whether a larger Δ_d is necessarily associated with the larger $\text{MO}_{6/2}$ site where bond-length segregation is found, we turn to structural data of Woodward *et al.*⁹ for CaFeO_3 , since this compound also undergoes a segregation below 290 K into two sets of $\text{FeO}_{6/2}$ octahedra of different bond lengths. In CaFeO_3 the transition at 290 K appears to be smooth, and Δ_d for both the smaller and larger $\text{FeO}_{6/2}$ octahedra is the same as that of RFeO_3 and the smaller $\text{NiO}_{6/2}$ octahedra. Only the introduction of a JT component to the distortion can

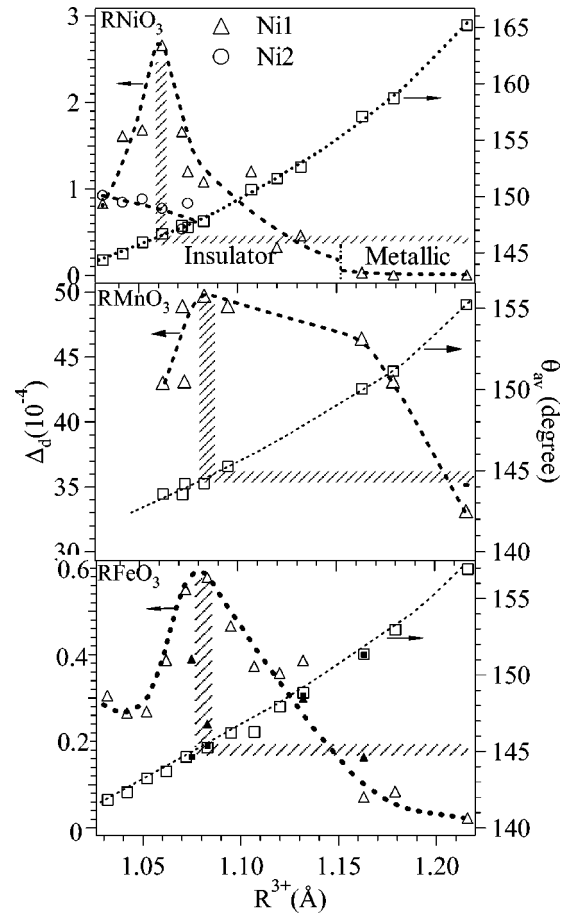


FIG. 3. The bonding distortion parameter Δ_d and the average angle θ_{av} of the M -O- M bond as a function of rare earth radii in RMO_3 . The data are from Refs. 3–7 and 12–17. The symbols of solid triangle and square represent structure data of RFeO_3 crystals from a synchrotron radiation source (Refs. 14–16). Alonso *et al.* (Ref. 17) attributed the decrease of Δ_d as the θ_{av} reduces further from about 145° to the presence of some Mn^{4+} . This argument does not make sense because creation of smaller Mn^{4+} in the RMnO_3 will relocate θ_{av} to a higher value that has not been seen in this case. There is an obvious printing error of the bond angle $\text{Fe}^{\text{II}}\text{-O(I)-Fe}^{\text{I}}$ for GdFeO_3 in the original report (Ref. 10). An average value of that in EuFeO_3 and TbFeO_3 has been used here.

account for an increase by a factor of 5 in the Δ_d of the larger $\text{NiO}_{6/2}$ octahedral site. The larger Δ_d at the $\text{NiO}_{6/2}$ octahedra with a longer $\langle \text{Ni-O} \rangle$ is more consistent with an ordering of more ionic and more covalent bonding at Ni^{3+} ions than with a charge disproportionation that would not introduce a different Δ_d at $\text{Ni}^{3+\delta}$ and $\text{Ni}^{3-\delta}$ ions.

Two factors reduce Δ_d at the more ionic $\text{NiO}_{6/2}$ sites relative to that for LaMnO_3 : stronger covalent bonding and a smaller concentration of JT ions. The Δ_d of the RMnO_3 family decreases as the size of the R^{3+} ion increases to La^{3+} , and we have argued elsewhere^{21,22} that LaMnO_3 approaches a transition from localized to itinerant electronic behavior from the localized-electron side. The greater the covalent component of the bonding, the smaller Δ_d . More important, however, are the elastic forces that limit the magnitude of the JT distortion and the cooperativity of the orbital ordering that

enhances the distortion. With only half of the $\text{NiO}_{6/2}$ octahedra in the RNiO_3 perovskites having localized e^1 configurations, the cooperativity is greatly reduced relative to the situation in LaMnO_3 , where every octahedral site has a localized e^1 configuration. As an example, the cooperativity in LaMnO_3 is reduced as the Mn^{3+} ions are diluted by Ga^{3+} ions.²³

Another remarkable feature of Fig. 3 is the maximum in Δ_d , which occurs at $\theta = 145 \pm 1^\circ$ in all three families of RMO_3 with $M = \text{Mn, Fe, Ni}$. The increase in Δ_d with increasing $\text{FeO}_{6/2}$ rotation, i.e., lower θ_{av} , in the RFeO_3 perovskites can only reflect the accommodation to improved bonding with the R^{3+} ion. Δ_d is magnified in RMnO_3 and the larger $\text{NiO}_{6/2}$ site of RNiO_3 by an ordering of the occupied e^1 orbitals. However, with or without the enhanced distortions, the magnitude of Δ_d is progressively lowered as $(145^\circ - \theta)$ increases. We note that the strength of the $(180^\circ - \phi)$ σ -bond M -O- M interactions decrease as $\langle \cos^2 \theta \rangle$ and that at $\theta = 145^\circ$ in the RMnO_3 family the magnetic order changes from type-A antiferromagnetic order to type-E antiferromagnetic order. The type-E antiferromagnetic order has been argued²⁴ to reflect the appearance of stronger M -O-O- M interactions between next-nearest neighbors than the $(180^\circ - \phi)$ M -O- M interactions between nearest neighbors in the RMnO_3 family. Therefore, the progressive decrease in Δ_d with increasing $(145^\circ - \theta)$ appears to be due to the onset of oxygen-oxygen interactions that are enhanced by spin polarization on the oxygen ions via their interaction with localized spins on the cations with which they bond.

This comparative study of the local octahedral-site distortions in the three RMO_3 perovskite families $M = \text{Mn, Fe, Ni}$ leads to the following conclusions: (1) Corresponding to the evolution from itinerant σ^* electrons of e -orbital parentage on metallic LaNiO_3 toward localized electronic behavior with smaller R^{3+} ions, there are four distinguishable Ni-O bond lengths as the θ_{av} changes over a broader range in RNiO_3 than that in RMO_3 ($M = \text{Fe, Mn}$). A vibronic bonding state at the crossover has been identified quantitatively along with the ionic, covalent and metallic bondings. (2) The typical ionic bond length and a significantly higher octahedral-site distortion in the larger $\text{NiO}_{6/2}$ octahedra than that in RFeO_3 indicates that the structural segregation into smaller and larger $\text{NiO}_{6/2}$ octahedra below $\theta = 147.5^\circ$ is associated with a segregation into more ionic and more covalent bonding rather than with a charge disproportionation. A JT localized-electron orbital ordering induces a distortion of the more ionic $\text{NiO}_{6/2}$ octahedra. (3) At a bending angle $\theta = 145^\circ$ of the M -O- M bond, the $(180^\circ - \phi)$ M -O- M σ -bond interactions compete with M -O-O- M interactions resulting from O-O interactions that are strengthened not only by the shorter O-O separation, but also by a spin polarization of the O-2 p electrons by interactions with localized spins on the neighboring cations.

The authors would like to thank the NSF, the TCSUH of Houston, Texas, and the Robert A. Welch Foundation of Houston, Texas for financial support.

- ¹J. B. Torrance, P. Lacorre, A. I. Nazzari, E. J. Ansaldo, and Ch. Niedermayer, *Phys. Rev. B* **45**, 8209 (1992).
- ²J.-S. Zhou, J. B. Goodenough, B. Dabrowski, P. W. Klamut, and Z. Bukowski, *Phys. Rev. Lett.* **84**, 526 (2000).
- ³J. A. Alonso, J. L. Garcia-Munoz, M. T. Fernandez-Diaz, M. A. G. Aranda, M. J. Martinez-Lope, and M. T. Casais, *Phys. Rev. Lett.* **82**, 3871 (1999).
- ⁴J. A. Alonso, M. J. Martinez-Lope, M. T. Casais, M. A. G. Aranda, and M. T. Fernandez-Diaz, *J. Am. Chem. Soc.* **121**, 4754 (1999).
- ⁵J. A. Alonso, M. J. Martinez-Lope, M. T. Casais, J. L. Martinez, G. Demazeau, A. Largeteau, J. L. Garcia-Munoz, A. Munoz, and M. T. Fernandez-Diaz, *Comput. Mater. Sci.* **11**, 2463 (1999).
- ⁶J. A. Alonso, M. J. Martinez-Lope, M. T. Casais, J. L. Garcia-Munoz, and M. T. Fernandez-Diaz, *Phys. Rev. B* **61**, 1756 (2000).
- ⁷J. A. Alonso, M. J. Martinez-Lope, M. T. Casais, J. L. Garcia-Munoz, M. T. Fernandez-Diaz, and M. A. G. Aranda, *Phys. Rev. B* **64**, 94102 (2001).
- ⁸J.-S. Zhou and J. B. Goodenough, *Phys. Rev. B* **60**, R15002 (1999).
- ⁹R. D. Shannon, *Acta Crystallogr., Sect. A: Cryst. Phys., Diffraction, Theor. Gen. Crystallogr.* **32**, 751 (1976).
- ¹⁰M. Marezio, J. P. Remeika, and P. D. Dernier, *Acta Crystallogr., Sect. B: Struct. Crystallogr. Cryst. Chem.* **26**, 2008 (1970).
- ¹¹C. Boekema, F. Van Der Woude, and G. A. Sawatzky, *Int. J. Magn.* **3**, 341 (1972).
- ¹²J. L. Garcia-Munoz, J. Rodriguez-Carvajal, P. Lacorre, and J. B. Torrance, *Phys. Rev. B* **46**, 4414 (1992).
- ¹³M. Marezio and P. D. Dernier, *Mater. Res. Bull.* **6**, 23 (1971).
- ¹⁴D. Du Boulay, E. N. Maslen, V. A. Streltsov, and N. Ishizawa, *Acta Crystallogr., Sect. B: Struct. Sci.* **51**, 921 (1995).
- ¹⁵E. N. Maslen, V. A. Streltsov, and N. Ishizawa, *Acta Crystallogr., Sect. B: Struct. Sci.* **52**, 406 (1996).
- ¹⁶V. A. Streltsov and N. Ishizawa, *Acta Crystallogr., Sect. B: Struct. Sci.* **55**, 1 (1999).
- ¹⁷J. A. Alonso, M. J. Martinez-Lope, M. T. Casais, and M. T. Fernandez-Diaz, *Inorg. Chem.* **39**, 917 (2000).
- ¹⁸M. Zaghrioui, A. Bulou, P. Lacorre, and P. Laffez, *Phys. Rev. B* **64**, 81102 (2001).
- ¹⁹J.-S. Zhou, J. B. Goodenough, and B. Dabrowski, *Phys. Rev. B* **67**, 20404 (2003).
- ²⁰D. B. McWhan, A. Menth, J. P. Remeika, W. F. Brinkman, and T. M. Rice, *Phys. Rev. B* **7**, 1920 (1973).
- ²¹J.-S. Zhou and J. B. Goodenough, *Phys. Rev. Lett.* **89**, 87201 (2002).
- ²²J.-S. Zhou and J. B. Goodenough, *Phys. Rev. B* **68**, 54403 (2003).
- ²³J.-S. Zhou and J. B. Goodenough, *Phys. Rev. B* **68**, 144406 (2003).
- ²⁴T. Kimura, S. Ishihara, H. Shintani, T. Arima, K. T. Takahashi, K. Ishizaka, and Y. Tokura, *Phys. Rev. B* **68**, R60403 (2003).
- ²⁵M. L. Medarde, *J. Phys.: Condens. Matter* **9**, 1679 (1997).